Inclusive $pp \to ZZ \to \ell^-\ell^+\nu\bar{\nu}$ full Run2 analysis report

Aleksandr Petukhov

National Research Nuclear University «MEPhI»
MEPhI@ATLAS meeting

28.04.2023

Motivation

$pp \to ZZ$ production is the rarest diboson process predicted by the **Standard Model (SM)**.

No ZZZ or $ZZ\gamma$ couplings at tree level of SM $\to$ indirect search of the effects predicted by the theories **beyond SM (BSM)**.

$pp \to ZZ \to \ell^-\ell^+\ell'^-\ell'^+ (\to \ell^-\ell^+\nu\bar{\nu})$ is an important background for on-shell (off-shell) **Higgs boson** production.

$ZZ \to \ell^-\ell^+\nu\bar{\nu}$ has a higher branching ratio than $ZZ \to \ell^-\ell^+\ell'^-\ell'^+$[1], but has a higher background contamination.
Worse cross section precision, better sensitivity for BSM processes at extreme values of Z boson p_T.
The hadron channel has the highest branching ratio, but is difficult to work with.

Allowed in SM

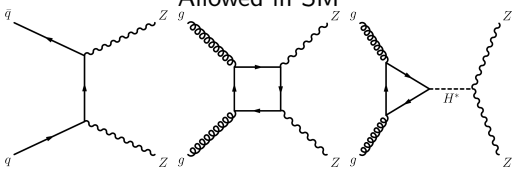

Not allowed in SM

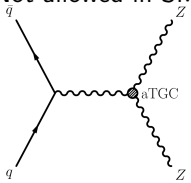

[1] $ZZ \to q\bar{q}$ (69.91%), $ZZ \to e^-e^+$ (3.36%), $ZZ \to \mu^-\mu^+$ (3.37%), $ZZ \to \nu\bar{\nu}$ (20.00%)

Motivation. Goals

Standard Model

Calculate integral and differential cross-sections in $\boldsymbol{p_{\mathrm{T}}^{Z}} = \boldsymbol{p_{\mathrm{T}}^{\ell\ell}}$, $\boldsymbol{\Delta\varphi(\ell\ell)}$, $\boldsymbol{m_{\mathrm{T}}^{ZZ}}$, $\boldsymbol{N_{\mathrm{jets}}}$, $\boldsymbol{m(j_1, j_2)}$
The results are to be compared to the theoretical prediction with NNLO corrections in α_s ([1], [2]) and NLO corrections in α_{EWK} ([3]).

Beyond Standard Model

Limits on the anomalous gauge-boson couplings (aTGCs) using vertex functions and EFT formalisms.

The same EFT coefficients as in the ongoing $Z(\nu\bar{\nu})\gamma$ analysis performed by MEPhI group (see Diana's presentation).
The $Z(\nu\bar{\nu})\gamma$ is expected to have more stringent limits as individual analysis, but the combination of two analyses would allow to improve them even further.

Previous $pp \to ZZ$ analyses

Paper	Public results	$\sqrt{s}$, TeV	Lumi, fb^{-1}	$2\ell 2\ell'$	$2\ell 2\nu$
		ATLAS			
JHEP 03 (2013) 128	STDM-2012-02	7	4.6	✓	✓
PLB 753 (2016) 552	STDM-2014-15	8	20.3	✓*	
Phys. Rev. Lett. 116 (2016) 101801	STDM-2015-13	13	3.2	✓	
JHEP 01 (2017) 099	STDM-2014-16	8	20.3	✓	✓
Phys. Rev. D 97 (2018) 032005	STDM-2016-15	13	36.1	✓	
JHEP 04 (2019) 048	STDM-2017-09	13	36.1	✓*	
JHEP 10 (2019) 127	STDM-2017-03	13	36.1		✓
JHEP 07 (2021) 005	STDM-2018-30	13	139	✓*	
		CMS			
JHEP 01 (2013) 063	SMP-12-007	7	5.0	✓	
EPJC 75 (2015) 511	SMP-12-016	7/8	5.1/19.6		✓
PLB 740 (2015) 250, PLB 757 (2016) 569	SMP-13-005	8	19.6	✓	
PLB 763 (2016) 280, PLB 772 (2017) 884	SMP-16-017	13	2.6	✓	
EPJC 78 (2018) 165, EPJC 78 (2018) 515	SMP-16-017	13	35.9	✓	
EPJC 81 (2021) 200	SMP-19-001	13	137	✓	

Analyses marked with ✓* study inclusive $pp \to 2\ell 2\ell'$ processes instead of $pp \to ZZ \to 2\ell 2\ell'$

I'll focus on results form the highlighted analyses.

Previous analyses. Comparison between $2\ell 2\nu$ and $2\ell 2\ell'$ channels.

Total $pp \to ZZ$ cross section with branching ratio taken into account.

Analysis	Cross section, pb	Uncertainty, pb					Rel. unc.
		stat	syst	lumi	theo	total	
ATLAS, 36.1 fb^{-1}, $2\ell 2\nu$	17,8	1	0,7	0,4		1,3	7,2%
ATLAS, 36.1 fb^{-1}, $2\ell 2\ell'$	17,3	0,6	0,5	0,6		1,0	5,7%
CMS, 35.9 fb^{-1}, $2\ell 2\ell'$	17,2	0,5	0,7	0,4	0,4	1,0	6,0%
CMS, 137 fb^{-1}, $2\ell 2\ell'$	17,4	0,3	0,5	0,3	0,4	0,8	4,4%

Analysis	Observed limits, [$\times 10^{-3}$]			
	f_4^γ	f_4^Z	f_5^γ	f_4^Z
ATLAS, 36.1 fb^{-1}, $2\ell 2\nu$	-1.2, 1.2	-1.0, 1.0	-1.2, 1.2	-1.0, 1.0
ATLAS, 36.1 fb^{-1}, $2\ell 2\ell'$	-1.8, 1.8	-1.5, 1.5	-1.8, 1.8	-1.5, 1.5
CMS, 35.9 fb^{-1}, $2\ell 2\ell'$	-1.2, 1.3	-1.2, 1.0	-1.2, 1.3	-1.2, 1.3
CMS, 137 fb^{-1}, $2\ell 2\ell'$	-0.78, 0.71	-0.66, 0.60	-0.68, 0.75	-0.55, 0.75

Worse accuracy for the integral cross section due to the higher cuts on the p_T of the second Z-boson.

Better BSM limits due to better statistics of the extreme Z boson p_T values.

ATLAS, 139 fb^{-1}, $2\ell 2\ell'$ doesn't measure the total $pp \to ZZ$ cross section or aTGCs.

Previous analyses. Differential cross section

Analysis	Variables used for differential cross section measurement							
ATLAS, 36.1 fb^{-1}, $2\ell 2\nu$	$m_T(ZZ)$	$p_T(ZZ)$	$p_T(\ell_1\ell_2)$	$p_T(\ell_1)$	$\lvert\Delta y(\ell\ell)\rvert$	$\lvert\Delta\varphi(\ell_1\ell_2)\rvert$	N_{jets}	$p_T(j_1)$
ATLAS, 36.1 fb^{-1}, $2\ell 2\ell'$		$p_T(ZZ)$	$p_T(\ell_1\ell_2)$	$p_T(\ell_{1,2,3,4})$			N_{jets}[2]	$p_T(j_{1,2})$
CMS, 35.9 fb^{-1}, $2\ell 2\ell'$		$p_T(ZZ)$	$p_T(\ell\ell)$	$p_T(\ell)$				
ATLAS, 139 fb^{-1}, $2\ell 2\ell'$			$p_T(\ell_1\ell_2)$			$\lvert\Delta\varphi(\ell_1\ell_2)\rvert$		
CMS, 137 fb^{-1}, $2\ell 2\ell'$		$p_T(ZZ)$	$p_T(\ell\ell)$	$p_T(\ell)$				

Analysis	Variables used for differential cross section measurement					
ATLAS, 36.1 fb^{-1}, $2\ell 2\nu$						
ATLAS, 36.1 fb^{-1}, $2\ell 2\ell'$	$\lvert\Delta\varphi(ZZ)\rvert$			$\lvert\eta(j_{1,2})\rvert$	$\lvert\Delta y(j_1, j_2)\rvert$	$m(j_1, j_2)$
CMS, 35.9 fb^{-1}, $2\ell 2\ell'$	$\lvert\Delta\varphi(ZZ)\rvert$					
ATLAS, 139 fb^{-1}, $2\ell 2\ell'$	$\lvert\Delta\varphi(ZZ)\rvert$	$m(\ell_1, \ell_2)$	$\cos\theta^*_{12}$[3]			
CMS, 137 fb^{-1}, $2\ell 2\ell'$	$\lvert\Delta\varphi(ZZ)\rvert$					

Only variables that are possible to be measured in the $2\ell 2\nu$ final state are presented in these tables.

[3] Also measured for jets with $|\eta| < 2.4$ and for jets with $p_T > 60$ GeV.

[3] θ^*_{12} is the angle between the negative lepton in the dilepton rest frame and the positive lepton in the laboratory frame. Sensitive to the polarization.

$p_T(\ell_1\ell_2)$ distributions

For $2\ell 2\ell'$ final state ATLAS papers *distinguish* the lepton pairs for the cross-section measurement.

ATLAS, 36.1 fb^{-1}, $2\ell 2\nu$

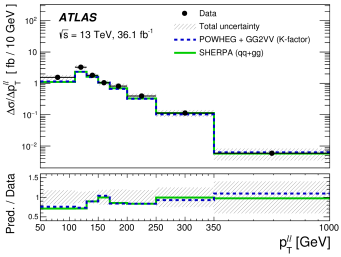

ATLAS, 36.1 fb^{-1}, $2\ell 2\ell'$

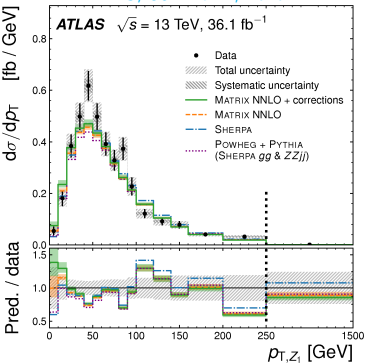

ATLAS, 139 fb^{-1}, $2\ell 2\ell'$

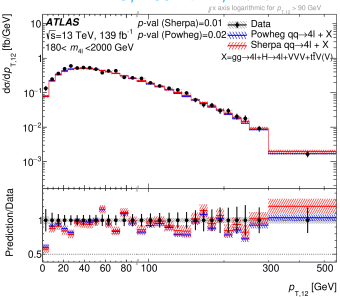

$p_T(\ell\ell)$ distributions

For $2\ell 2\ell'$ final state CMS papers *combine* the lepton pairs for the cross-section measurement.

CMS, 35.9 fb^{-1}, $2\ell 2\ell'$

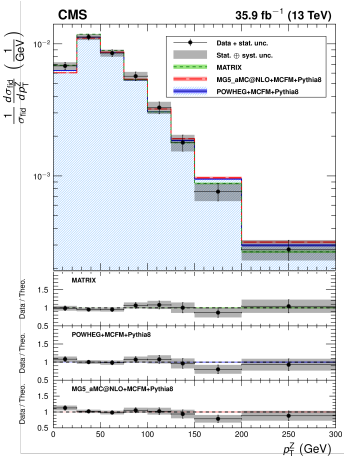

CMS, 137 fb^{-1}, $2\ell 2\ell'$

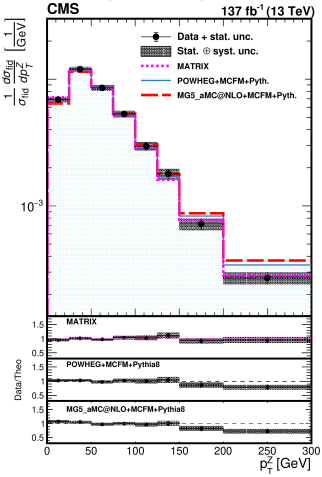

Previous analyses. BSM limits

Limit setting on the effects of the physics beyond the Standard model is performed in two formalisms:
aTGC parameters: f_4^γ, f_4^Z, f_5^γ, f_4^Z
EFT parameters, dimension-8: $C_{\tilde{B}W}/\Lambda^4$, C_{WW}/Λ^4, C_{BW}/Λ^4, C_{BB}/Λ^4

	aTGC	EFT
ATLAS, 36.1 fb^{-1}, $2\ell 2\nu$	✓	
ATLAS, 36.1 fb^{-1}, $2\ell 2\ell'$	✓	✓
CMS, 35.9 fb^{-1}, $2\ell 2\ell'$	✓	
CMS, 137 fb^{-1}, $2\ell 2\ell'$	✓	✓

Analysis	Observed limits, [$\times 10^{-3}$]			
	f_4^γ	f_4^Z	f_5^γ	f_4^Z
ATLAS, 36.1 fb^{-1}, $2\ell 2\nu$	-1.2, 1.2	-1.0, 1.0	-1.2, 1.2	-1.0, 1.0
ATLAS, 36.1 fb^{-1}, $2\ell 2\ell'$	-1.8, 1.8	-1.5, 1.5	-1.8, 1.8	-1.5, 1.5
CMS, 35.9 fb^{-1}, $2\ell 2\ell'$	-1.2, 1.3	-1.2, 1.0	-1.2, 1.3	-1.2, 1.3
CMS, 137 fb^{-1}, $2\ell 2\ell'$	-0.78, 0.71	-0.66, 0.60	-0.68, 0.75	-0.55, 0.75

ATLAS, 139 fb^{-1}, $2\ell 2\ell'$ doesn't measure the aTGCs and only measures dimension-6 EFT operator couplings, as it is more sensitive to them.

Selection optimization

Topology: pair of same flavour opposite sign leptons (e or μ) + high missing transverse momentum $E_{\mathrm{T}}^{\mathrm{miss}}$.

Preselection	Cut value
N_{leptons}	$= 2$
$p_{\mathrm{T}}(\ell_1)$, GeV	> 30
$p_{\mathrm{T}}(\ell_2)$, GeV	> 20
$m_{\ell\ell}$, GeV	$\in [76; 106]$
$E_{\mathrm{T}}^{\mathrm{miss}}$, GeV	> 70

Detailed object selection criteria could be found in the backup slides.

The final signal region selection is performed by grid search over the following variables[4]: $E_{\mathrm{T}}^{\mathrm{miss}}$, $\Delta R(\ell\ell)$, $\Delta\varphi(\vec{p}_T^{\,\mathrm{miss}}, \vec{p}_T^{\,\ell\ell})$, $E_{\mathrm{T}}^{\mathrm{miss}}/H_{\mathrm{T}}$[5], $N_{\text{b-jets}}$.

Fixed cut approach or tight selection.
Maximize estimation of the statistical significance Z

MVA approach or loose selection
Maximize estimation of the statistical significance Z and $S > 3000$.

$$Z = \sqrt{2\left((S+B)\cdot \ln\left(1+\frac{S}{B}\right) - S\right)}$$

[5] Grid steps could be found in the backup slides

[5] $H_{\mathrm{T}} = p_{\mathrm{T}}(\ell_1) + p_{\mathrm{T}}(\ell_2) + \sum_i p_{\mathrm{T}}(j_i)$ — scalar sum of p_{T} of both leptons and all jest passing the selection criteria.

Signal region selection

The optimization yields the following selections.
Additional $m_{\ell\ell}$ was added for the **strict** selection as it increased the estimate of the statistical significance.

	Strict	**Loose**
$m_{\ell\ell}$, GeV	$\in [80; 100]$	$\in [76; 106]$
$E_{\mathrm{T}}^{\mathrm{miss}}$, GeV	> 110	> 90
$\Delta R(\ell\ell)$	< 1.8	< 2.2
$\Delta\varphi(\vec{p}_T^{\mathrm{miss}}, \vec{p}_T^{\ell\ell})$	> 2.7	> 1.3
$E_{\mathrm{T}}^{\mathrm{miss}}/H_{\mathrm{T}}$	> 0.65	> 0.1
$N_{\text{b-jets}}$	$= 0$	$= 0$

	Strict	**Loose**
Signal	1562 ± 15	3810 ± 20
Background	1007 ± 17	25000 ± 300
Significance	41.1	23.5

The following slides will report on the studies for the fixed cut approach using **strict** signal region definition.

Background composition

Process	% of background	
	Strict	**Loose**
$WZ \to \ell\nu\ell\ell$ — one missing ℓ mimics the signal topology	68%	12%
$Z(\to \ell\ell) + \text{jets}$ — lepton pair with mismeasured $E_{\mathrm{T}}^{\mathrm{miss}}$	15%	69%
$WW \to \ell\nu\ell'\nu'$ — non resonant production of a lepton pair	3%	3%
Wt, t, $t\bar{t}$, ttV — non resonant production of a lepton pair via t-quark	9%	15%
Other backgrounds: 4ℓ, $\ell\ell qq$, VVV, $Z(\tau\tau)$, $W + \text{jets}$	5%	1%

All of the backgrounds (except for "Other"):

- Normalized in a simultaneous fit with the shape taken from Monte-Carlo (**main method**).
- Normalization is cross-checked with data-driven approaches (auxiliary method).

$Z(\to \ell\ell) +$ **jets** is additionally split by decay (ee and $\mu\mu$) and number of jets (0, 1, ≥ 2) to better recreate the shape.

Fit description

The integral cross-section and the backgrounds are estimated in the **maximum likelihood fit**, by maximizing the following function in terms of μ and η:

$$\mathcal{L}(\mu,\theta) = \prod_{r}^{\text{regions}} \left[\prod_{i}^{\text{bins}\in r} \text{Pois}(N_i^{\text{data}} | \mu\nu_i^s\eta^s(\theta) + \nu_i^b\eta^b(\theta)) \right] \cdot \prod_{i}^{\text{nuis. par.}} \mathcal{L}(\theta_i),$$

N (ν) — observed (predicted) event yields
μ — signal normalization coefficient (signal strength), $\mu = \nu^s/N^s$.
θ — background normalization coefficients and systematic uncertainties nuisance parameters.
η — parameterize effect of θ on the predicted yields.

The fit has 10 regions (including signal region) and 10 normalization coefficients (including signal strength).
All of the regions use $\Delta\varphi(\vec{p}_T^{\text{miss}}, \vec{p}_T^{\ell\ell})$ distribution.

Right now fit to the observed data is performed **only in control regions**.

$WZ \to \ell'\nu\ell\ell$ background

$Z \to \ell\ell$, where $\ell = e, \mu$
$W \to \ell'\nu$, where $\ell' = e, \mu, \tau$

Genuine $E_{\mathrm{T}}^{\mathrm{miss}}$ from the W boson decay, one of the 3 charged leptons escapes detection.

Control region (called 3ℓ **CR**) is created by requiring:

- one additional lepton ($N_{\mathrm{leptons}} = 3$).
- $m_{\mathrm{T}}^{W} > 30$ GeV, where $m_{\mathrm{T}}^{W} = \sqrt{2 p_T^{\ell 3} E_{\mathrm{T}}^{\mathrm{miss}} \left[1 - \cos\left(\Delta\phi\left(p_T^{\ell 3}, E_{\mathrm{T}}^{\mathrm{miss}}\right)\right)\right]}$.

Normalization is estimated in the fit using $\mu(WZ)$ normalization coefficient.

Non-resonant backgrounds

Genuine $\ell\ell\nu\nu$ in the final state with the charged leptons coming from the different particle decays. WW, Wt, t, $t\bar{t}$, ttV processes.

Control region (called **non-res. CR**) is constructed by requiring the lepton pair to have different flavour, i.e. $e^{\pm}\mu^{\mp}$.
The CR is further separated in two categories:

1. $N_{\text{b-jets}} = 0$ with main contribution from the WW process.
2. $N_{\text{b-jets}} > 1$ with main contribution from the Wt, t, $t\bar{t}$, ttV processes.

Normalization is estimated in the fit using two normalization coefficients:

1. $\mu(WW)$ for the WW process.
2. $\mu(\text{top})$ for the Wt, t, $t\bar{t}$, ttV processes.

Z + jets background

$Z \to \ell\ell$ + mismeasured $E_{\mathrm{T}}^{\mathrm{miss}}$.

Control region (called Z+**jets CR**) is constructed by inverting the $E_{\mathrm{T}}^{\mathrm{miss}}$ and $E_{\mathrm{T}}^{\mathrm{miss}}/H_{\mathrm{T}}$ cuts of the SR

$(E_{\mathrm{T}}^{\mathrm{miss}} \in [70; 80]$ GeV & $E_{\mathrm{T}}^{\mathrm{miss}}/H_{\mathrm{T}} > 0.3)$ ||
$(E_{\mathrm{T}}^{\mathrm{miss}} > 80$ GeV & $E_{\mathrm{T}}^{\mathrm{miss}}/H_{\mathrm{T}} < [0.3; 0.45])$

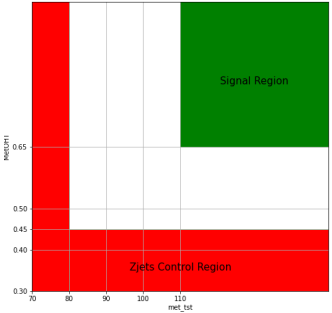

To properly reproduce the shape of the background in the SR it is estimated using 6 normalization coefficients by splitting the Z + jets into 6 categories by:

- N_{jets} into categories with 0, 1 and ≥ 2 jets.
- lepton pair flavour into categories with ee and $\mu\mu$.

Each part of the Z + jets is estimated in a dedicated control region.

Fit region definition

	SR	3ℓ CR	Non-res. CR	Z+jets CR
$m_{\ell\ell}$, GeV	$\in [80; 100]$	$\in [80; 100]$	$\in [80; 100]$	$\in [80; 100]$
$E_{\mathrm{T}}^{\mathrm{miss}}$, GeV	> 110	> 70	> 70	See figure
$\Delta R(\ell\ell)$	< 1.8	< 2	< 2	< 1.8
$\Delta\varphi(\vec{p}_T^{\,\mathrm{miss}}, \vec{p}_T^{\,\ell\ell})$	> 2.7	> 2.2	> 2.2	> 2.2
$E_{\mathrm{T}}^{\mathrm{miss}}/H_{\mathrm{T}}$	> 0.65	> 0.3	> 0.3	See figure
$N_{\text{b-jets}}$	$= 0$	$= 0$	$\{0; \geq 1\}$	$= 0$
N_{jets}	≥ 0	≥ 0	≥ 0	$\{0; 1; \geq 2\}$
Lepton pair flavour	SFOC	SFOC	$e^{\pm}\mu^{\mp}$	$\{ee; \mu\mu\}$
N_{leptons}	$= 2$	$= 3$	$= 2$	$= 2$
m_{T}^{W}, GeV	—	> 30	—	—

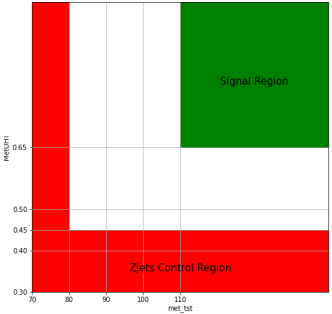

3ℓ CR

Has an additional lepton and a cut on $m_{\mathrm{T}}^{W} = \sqrt{2p_T^{\ell 3} E_{\mathrm{T}}^{\mathrm{miss}} \left[1 - \cos\left(\Delta\phi\left(p_T^{\ell 3}, E_{\mathrm{T}}^{\mathrm{miss}}\right)\right)\right]}$

Non-res. CR

Has a opposite flavour opposite charge lepton pair and split into 2 categories by $N_{\text{b-jets}}$

Z+jets CR

Has a complex definition of ($E_{\mathrm{T}}^{\mathrm{miss}} \in [70; 80]$ GeV & $E_{\mathrm{T}}^{\mathrm{miss}}/H_{\mathrm{T}} > 0.3$) $\parallel$ ($E_{\mathrm{T}}^{\mathrm{miss}} > 80$ GeV & $E_{\mathrm{T}}^{\mathrm{miss}}/H_{\mathrm{T}} < [0.3; 0.45]$).
Split into 6 categories by N_{jets} and lepton pair flavour.

Pre-fit distibutions. *WZ* and non-resonant backgrounds.

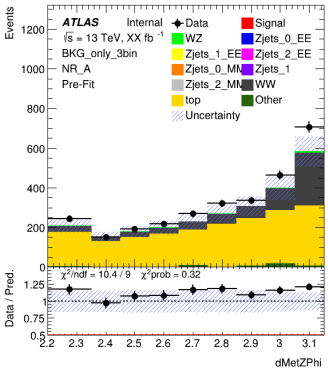

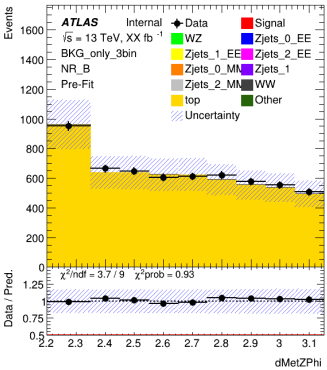

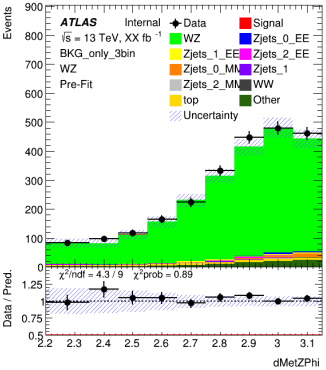

Pre-fit distibutions. Z+jets backgrounds.

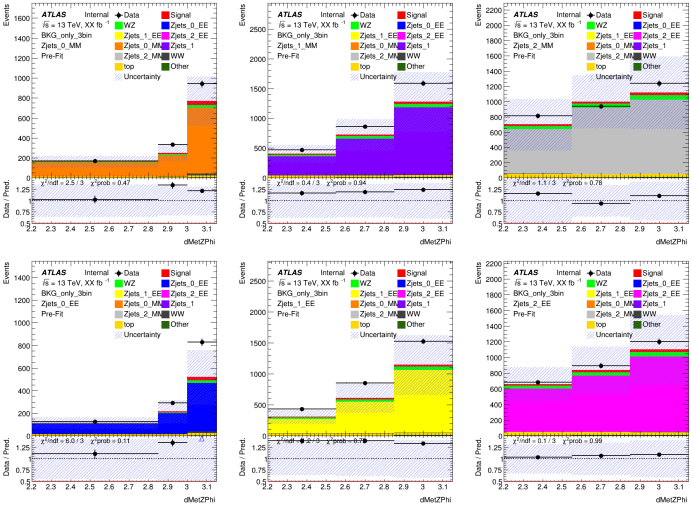

Post-fit distibutions. *WZ* and non-resonant backgrounds.

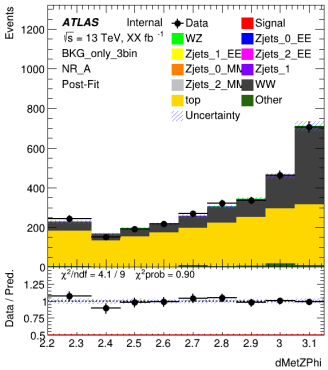

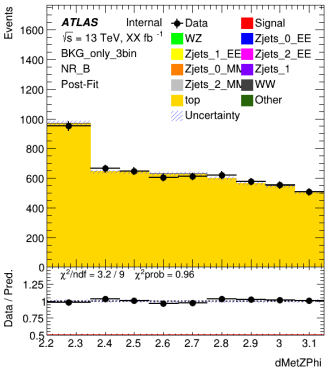

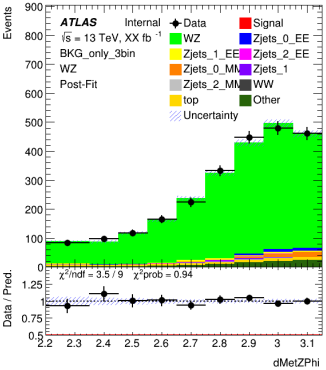

Post-fit distibutions. Z+jets backgrounds.

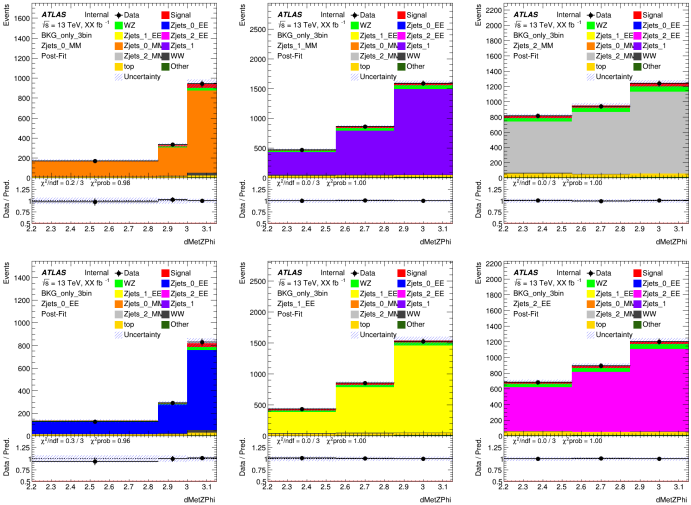

Normalization coefficients

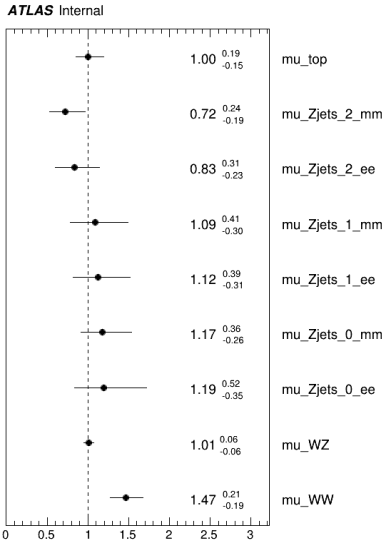

Object selection

Electrons

- Likehood medium
- p_T lead > 30 ГэВ
- p_T sublead > 20 ГэВ
- $|\eta|$ calo cluster < 2.47
- $|\Delta(z_0) \cdot \sin(\theta)| < 0.5$ мм
- $|d_0\text{-significance}| < 5$
- Isolation WP `FixedCutLoose`
- Crack region veto
- Исключение пересечений с мюонами и струями

Muons

- Medium
- $|\eta| < 2.5$
- p_T lead > 30 ГэВ
- p_T sublead > 20 ГэВ
- Combined muons
- $|\Delta(z_0) \cdot \sin(\theta)| < 0.5$ мм
- $|d_0\text{-significance}| < 3$
- Isolation WP `PflowLoose_FixedRad`
- Исключение пересечений со струями

Jets

- AntiKt4EMPFlow
- $p_T > 30$ ГэВ
- $|\eta| < 4.5$
- JVT > 0.5
- Event-level cleaning for LooseBad jets

E_T^{miss}

- Tight WP, rebuilt with METMaker using selected leptons and all calibrated jets

Selection optimization details

- $E_{\mathrm{T}}^{\mathrm{miss}}$, $[50; 1500]$ GeV, a step of 10 GeV;
- $\Delta R(\ell\ell)$, $[0; 4]$, a step of 0.1;
- $\Delta\varphi(\vec{p}_T^{\,\mathrm{miss}}, \vec{p}_T^{\,\ell\ell})$, $[0; 3.15]$, a step of 0.1;
- $E_{\mathrm{T}}^{\mathrm{miss}}/H_{\mathrm{T}}$, $[0; 2]$, a step of 0.05;
- $N_{\text{b-jets}}$, events with $\{0, 1, 2, 3, \geq 4\}$ b-jets.